ASSESSMENT OF TRABECULAR BONE MICRODAMAGE AND MICROFRACTURE

Srinidhi Nagaraja (1), Andres Laib (2), Robert E. Guldberg (1)

(1) School of Mechanical Engineering
Georgia Institute of Technology
Atlanta, GA

(2) Scanco Medical AG
Bassersdorf, Switzerland

INTRODUCTION

The onset of trabecular bone damage is a local phenomenon, governed by tissue-level material properties, and architecture at the initiation site. Different modes of microfracture (bending, buckling, and shearing) and microdamage (single, parallel, and cross-hatched cracks) can occur [1]. The initiation of bone damage can lead to two scenarios. In the first case, normal repair processes and/or bone remodeling result in replacement of the damaged region without loss of structural integrity. However, an accumulation of unrepaired microdamage with age or disease may increase bone fragility and lead to bone fracture. Although trabecular bone microdamage has great clinical relevance, the microstructural stresses and strains associated with local failure within trabecular bone are not well known. A better understanding of local mechanisms of bone failure is important to the improvement of fracture risk assessment and the development of therapies for bone fragility diseases such as osteoporosis. The purpose of this study was to use histological damage labeling, microcomputed tomography (micro-CT) imaging, and voxel-based finite element modeling to detect trabecular bone microdamage and microfracture and estimate the associated microstructural stresses and strains.

METHODS

Cylindrical reduced-section specimens were prepared from skeletally mature bovine proximal tibial trabecular bone [2]. End artifacts were minimized by attaching stainless steel endcaps to each end of the specimen using cyanoacrylate. The final reduced-section specimen had a 5 mm gauge length and 3 mm diameter. Specimens were randomly placed into four test groups. Group A underwent sequential compression steps of 0% and 0.75%. Group B underwent sequential compression steps of 0%, 0.75%, and 1.5%. Group C underwent sequential compression steps of 0%, 0.75%, 1.5%, and 2.25%. Group D underwent sequential compression steps of 0%, 0.75%, 1.5%, 2.25%, and 3%. In each group, the specimens were imaged after each strain step.

Prior to mechanical testing, specimens were stained with 0.03% alazarin complexone to label preexisting microdamage. After testing, specimens were stained with 0.01% calcein to label microdamage incurred from mechanical testing. The sequential labeling technique has been previously used to detect microdamage [3]. This technique differentiates preexisting damage from damage sustained by mechanical testing. After staining, specimens were embedded in poly (methyl)methacrylate (PMMA) and sectioned into longitudinal slices 200 μm thick on a diamond saw. Sections were observed under ultraviolet epifluorescence to detect the number and types of damage (single, parallel, cross-hatched, and complete fractures). A microfracture assessment script was developed to quantify trabecular fractures incurred during mechanical testing from micro-CT data. The script produced two segmentations of an image, one at high threshold and another at a low threshold. These images were then subtracted from each other to isolate fractured trabeculi in three-dimensional space.

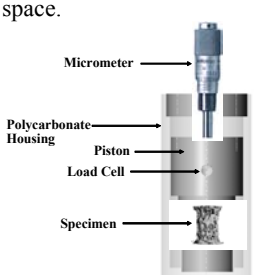

Figure 1. Schematic of Compressive Mechanical Testing System

Micro-CT images were acquired at various levels of static compression in a miniature compressive mechanical testing system. This system was designed to introduce stepwise uniaxial strains to the specimen while fitting within the micro-CT system (μCT 40 Scanco USA). As shown in Figure 1, apparent uniaxial strains were applied using a micrometer head (Mitutoyo Corp. USA) and an on-board subminiature load cell (Sensotech, USA) measured the compressive force. The miniature compressive testing system produced a similar stress-strain curve to a standard materials testing system (858 Mini

Bionix II MTS USA), validating the system's capability to apply uniaxial strains to a specimen.

Micro-CT images at the undeformed state (0% strain condition) were used as a basis for predicting the local stress and strain distribution using voxel-based finite element modeling. After thresholding the micro-CT image, individual voxels within the image were directly converted into hexahedral finite elements by assigning nodal connectivity and bone tissue properties. Trabecular bone properties were assumed to be 11.4 GPa and Poisson's ratio of 0.3 [4]. Boundary conditions replicating the mechanical test were imposed on the model. A linear finite element analysis using iterative equation solvers allowed for the estimation of tissue-level stresses and strains.

RESULTS

To assess the magnitude of microdamage and fracture, three approaches were taken. First, high levels of damage such as microfractures were quantified using micro-CT images. An automated microfracture detection program produced 3D images of complete fractures. The program quantified the number of microfractures and the total crack volume incurred from mechanical testing. As shown in Figure 2, a specimen from group D developed 18 additional microfracture sites when loaded from 0% to 3% strain.

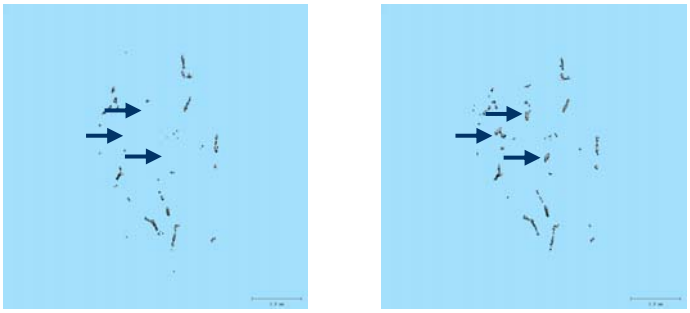

Figure 2. Micro-CT images of preexisting microfracture sites at 0% strain (left) and additional microfractures incurred when loaded to 3% strain (right).

Image-based finite element analysis was utilized to estimate local principal stresses corresponding to microfracture sites. As shown in Figure 3, a three-dimensional finite element model consisting of 1.4 million elements (20μm/element) was generated. A 3% uniaxial compressive strain was applied on the top face while the bottom face was fully constrained. Analyzing specific trabeculae demonstrated that estimated highly stressed trabeculi shown in red are fractured when compressed to 3% strain. For this sample, local tissue level yield was first detected between 1.5% and 2.25% strain as visualized by micro-CT images. However, apparent-level yield of the specimen occurred between 2.25% and 3%. The estimated local principal yield stress for the longitudinal failed trabeculae (Figure 3A) ranged from 159.2-238.8 MPa compressive stress. The corresponding estimated local principal yield strain was 0.73-0.91%. The estimated local principal yield stress for the horizontal failed trabeculae (Figure 3B) in the inset ranged from 178.1-222.6 MPa compressive stress. The corresponding estimated local principal yield strain was 0.71-0.88%.

Microdamage in the form of single, parallel, and cross-hatched cracks was detected using histological damage labeling. Histology sections using the sequential labeling technique were registered to estimated stress levels for the same section.

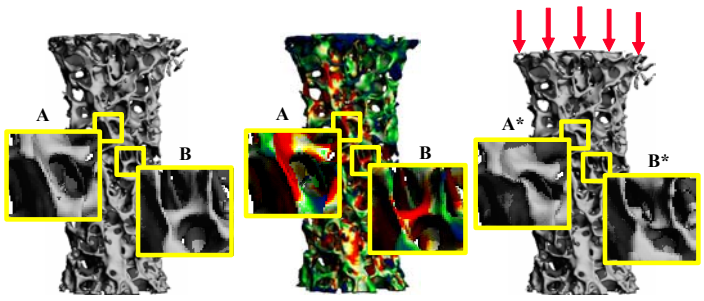

Figure 3. Microstructural failure analysis of trabecular bone. Micro-CT image of specimen in undeformed state (left), finite element model with Von-Mises stress distribution (middle), and micro-CT image compressed to 3% strain (right).

Under ultraviolet epifluorescence (20x magnification), preexisting damage fluoresced red and mechanical test induced damaged fluoresced green. As shown in Figure 4, areas of moderate stress concentrations matched well with site-specific diffuse damage, but not fracture.

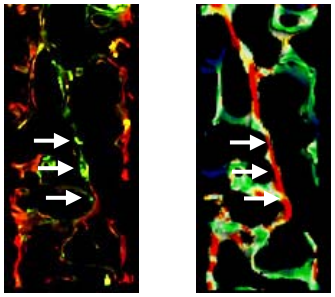

Figure 4. Analysis of microdamage within trabeculae. Histology section under epifluorescence (left) and finite element section with Von-Mises stress distribution (right).

DISCUSSSION

In order to track the progression of deformation and damage, a mechanical testing device that applied stepwise compressive strains to trabecular bone while being scanned in the micro-CT was designed and validated. Local estimated principal yield stress and strain for the longitudinal trabeculae are in good agreement with 133-193 MPa and 0.71-1.10% ranges previously reported for cortical bone [5]. Stresses in trabeculae A, which was aligned with the axis of loading, were entirely compressive; whereas, stresses in horizontal trabeculae B were both tensile and compressive, consistent with failure in bending and shear. Future work involves analyzing additional specimens to demonstrate correlations between microdamage and microstructural stresses and strains. Extension of these methods to human trabecular bone may allow local failure criterion to be developed as a function of age and disease.

ACKNOWLEDGEMENTS

Funding provided by NSF (EEC-9731643) and the micro-CT system was provided by an NSF Major Research Instrumentation Award (9977551).

REFERENCES

1. Burr, D.B. et al., 1997, J. Bone and Miner. Res. 12(1), pp. 6-13.
2. Keaveny, T.M. and McMahon, T.A., 1994, J. Biomech. 27(9), pp. 1127-1136.
3. Lee, T.C. et al., 2000, J. Orthop. Res. 18, pp. 322-325.
4. Zysset P.K. et al., 1999, J. Biomech. 32, pp. 1005-1012.
5. Burstein, A.H. et al., 1976, J. Bone Joint Surg. 31, pp. 82-86.